A SURFACE INTEGRAL EQUATION METHOD FOR EM MODELLING

John Doherty

Introduction

Since the early seventies, integral equations have been used in solving the boundary value problems that arise in the course of using either natural or artificial EM fields for studying earth structure. However the use of thick-body surface integral equation (SIE) techniques, in which the effect of a scatterer is represented by a surficial distribution of tangential electric and magnetic dipole moment density has been limited. There has been some theoretical treatment given to the method in the Russian literature (Dmitriev and Zakharov 1970; Tabarovsky 1975), but numerical results have been published only by Parry and Ward (1971), and Won and Kuo (1975), who each applied the technique to the case of the excitation of a 2-D body by a 2-D field, though both confined their numerical examples to the E-polarization case (electric field parallel to the conductor axis).

The 3-D Case—Mathematical Formulation

The situation is shown in Fig. 1 where a scatterer is placed in a full-space; (the layered half-space case is discussed later). Designate the primary fields as E_p and H_p, and let $\mathbf{E}_2$, $\mathbf{H}_1$ represent the secondary fields in region 1, and $\mathbf{E}_2$, $\mathbf{H}_2$ represent the secondary fields in region 2. With an exp $(-i\omega t)$ time dependence, it is assumed that these fields can be described as follows:

$$\mathbf{E}_1(\mathbf{r}) = i\omega\mu_1 \operatorname{curl} \int_{\partial D} \Phi_1(\mathbf{r},\mathbf{r}')\mathbf{b}(\mathbf{r}')ds(\mathbf{r}') + \operatorname{curl}\operatorname{curl} \int_{\partial D} \Phi_1(\mathbf{r},\mathbf{r}')\mathbf{a}(\mathbf{r}')ds(\mathbf{r}'), \quad (\mathbf{r} \in R^3\backslash D) \quad (1)$$

$$\mathbf{H}_1(\mathbf{r}) = (\sigma_1 - i\omega\epsilon_1) \operatorname{curl} \int_{\partial D} \Phi_1(\mathbf{r},\mathbf{r}')\mathbf{a}(\mathbf{r}')ds(\mathbf{r}') + \operatorname{curl}\operatorname{curl} \int_{\partial D} \Phi_1(\mathbf{r},\mathbf{r}')\mathbf{b}(\mathbf{r}')ds(\mathbf{r}'), \quad (\mathbf{r} \in R^3\backslash D) \quad (2)$$

$$\mathbf{E}_2(\mathbf{r}) = i\omega\mu_2 \operatorname{curl} \int_{\partial D} \Phi_2(\mathbf{r},\mathbf{r}')\mathbf{b}(\mathbf{r}')ds(\mathbf{r}') + \operatorname{curl}\operatorname{curl} \int_{\partial D} \Phi_2(\mathbf{r},\mathbf{r}')\mathbf{a}(\mathbf{r}')ds(\mathbf{r}'), \quad (\mathbf{r} \in D) \quad (3)$$

$$\mathbf{H}_2(\mathbf{r}) = (\sigma_2 - i\omega\epsilon_2) \operatorname{curl} \int_{\partial D} \Phi_2(\mathbf{r},\mathbf{r}')\mathbf{a}(\mathbf{r}')ds(\mathbf{r}') + \operatorname{curl}\operatorname{curl} \int_{\partial D} \Phi_2(\mathbf{r},\mathbf{r}')\mathbf{b}(\mathbf{r}')ds(\mathbf{r}') \quad (\mathbf{r} \in D) \quad (4)$$

where $\mathbf{a}$ and $\mathbf{b}$ are tangential vector fields, $\Phi(\mathbf{r},\mathbf{r}') = \exp(ik_i|\mathbf{r}-\mathbf{r}'|)/4\pi|\mathbf{r}-\mathbf{r}'|$, and $k_i^2 = i\omega\mu_i(\sigma_i - i\omega\epsilon_i)$.

If these fields are constrained to obey the boundary conditions at the scatterer surface, the following surface integral equations result:

$$[(\sigma_1 - i\omega\epsilon_1) + (\sigma_2 - i\omega\epsilon_2)]\mathbf{a}(\mathbf{r}) + 2\boldsymbol{\nu}(\mathbf{r}) \times \operatorname{curl} \int_{\partial D} [(\sigma_1 - i\omega\epsilon_1)\Phi_1(\mathbf{r},\mathbf{r}') - (\sigma_2 - i\omega\epsilon_2)\Phi_2(\mathbf{r},\mathbf{r}')]\mathbf{a}(\mathbf{r}')ds(\mathbf{r}') + 2\boldsymbol{\nu}(\mathbf{r}) \times \operatorname{curl}\operatorname{curl} \int_{\partial D} [\Phi_1(\mathbf{r},\mathbf{r}') - \Phi_2(\mathbf{r},\mathbf{r}')]\mathbf{b}(\mathbf{r}')ds(\mathbf{r}') = -2\boldsymbol{\nu}(\mathbf{r}) \times \mathbf{H}_p(\mathbf{r}), \quad (\mathbf{r} \in \partial D) \quad (5)$$

$$i\omega(\mu_1 + \mu_2)\mathbf{b}(\mathbf{r}) + 2\boldsymbol{\nu}(\mathbf{r}) \times \operatorname{curl}\operatorname{curl} \int_{\partial D} [\Phi_1(\mathbf{r},\mathbf{r}') - \Phi_2(\mathbf{r},\mathbf{r}')]\mathbf{a}(\mathbf{r}')ds(\mathbf{r}') + 2i\omega \operatorname{curl} \int_{\partial D} [\mu_1\Phi_1(\mathbf{r},\mathbf{r}') - \mu_2\Phi_2(\mathbf{r},\mathbf{r}')]\mathbf{b}(\mathbf{r}')ds(\mathbf{r}') = -2\boldsymbol{\nu}(\mathbf{r}) \times \mathbf{E}_p(\mathbf{r}), \quad (\mathbf{r} \in \partial D) \quad (6)$$

With an appropriate definition of function space, this system can be shown to form a Fredholm linear equation of the second kind involving a compact (in the linear systems sense) operator. (For a discussion of integral operators in scattering theory, see Colton and Kress 1983.) Hence the Riesz Theory can be invoked, together with the Uniqueness Theorem for the transmission boundary value problem, to show that a solution to this system for $\mathbf{a}$ and $\mathbf{b}$ exists, and is unique. Once the system is solved, the fields anywhere can then be found using eqns (1)–(4).

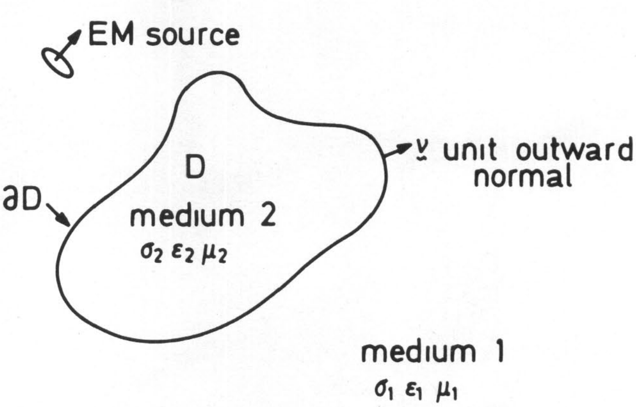

FIGURE 1
D is a bounded open region with boundary ∂D.

3-D Source, 2-D Body

Numerical results for the case of the scattering by an infinitely elongate body of the fields due to a finite source have so far been obtained in the EM context using the finite difference technique (Stoyer and Greenfield 1976), and the finite element technique (Stodt 1978; Lee and Morrison 1985). Also, formulations for special cases have been presented by Howard (1975); Tsubota and Wait (1980); Mahmoud *et al* (1981); and Hanneson and West (1984).

The SIE technique presented above can be adapted to this context by Fourier transforming eqns (5) and (6), solving for the transformed dipole moment densities, and using the transforms of eqns (1) to (4) to obtain the transformed EM fields at the desired field points, for each of a number of wavenumbers in the direction of elongation of the scatterer. These are then inverse Fourier transformed to obtain the fields at these points.

In the transform domain, the surface integrals become contour integrals, and eqns (5) and (6) become four simultaneous integral equations in four scaler unknowns, viz the components of each of the dipole moment densities both in the elongation direction and in the direction tangential to the surface cross-sectional contour.

2-D Scatterer in a Layered Half-Space

When the scatterer is not situated in a full space, the contribution from fields reflected from surrounding obstacles must be added to the transforms of expressions (1) and (2) for the fields outside the scatterer, and to the SIE resulting from enforcement of the boundary conditions. In the case of layered media, these expressions are available as the inverse Fourier transforms (IFT) of the secondary double transforms, the latter having an algebraic form involving a recursion formula (see, for example, Wannamaker *et al* 1984).

The method chosen to carry out the thousands of IFT's required in the course of solving the system of equations, is to express each IFT as a sine and cosine transform, and then to evaluate these by digital filtering. For example, defining the cosine transform as:

$$\hat{f}_c(x) = \int_0^\infty f(k_x)\cos(k_x x)dk_x$$

the change of variables $x = \mathrm{e}^{\nu}$ and $k_x = \mathrm{e}^{-u}$ yields the expression:

$$\{\mathrm{e}^{\nu/2}\hat{f}_c(\mathrm{e}^{\nu})\} = \int_{-\infty}^{\infty}\{\mathrm{e}^{-u/2}f(\mathrm{e}^{-u})\}\{\mathrm{e}^{(\nu-u)/2}\cos(\mathrm{e}^{\nu-u})\}du \quad (7)$$

This is a convolution integral, and hence repeated integrations can be performed with an appropriate set of filter coefficients. In the present study, sine and cosine coefficients, each at intervals of 10/decade and 15/decade, were calculated using the method described by Anderson (1979), for the determination of Hankel transform coefficients. Accuracy of integrations carried out using these coefficients depends on the functions being transformed, but appears to be best expressed as a fraction of the maximum value of the transform over its range. For the double Fourier transforms of the layered-earth secondary fields, accuracies of better then 10^{-5} are achieved with the 10/decade coefficients for most fields in most situations; this accuracy is increased by a factor of 2 if the 15/decade coefficients are used.

It should be noted that Johansen and Sorensen (1979), determined a set of coefficients for the convolution expressed by eqn. (7) using analytical expressions for them, while Anderson (1975) has also calculated a set of sine and cosine transform coefficients, but his filtering and input functions differed slightly from those shown in eqn. (7).

A Numerical Result — 3-D Source, 2-D Body in a Half-Space

Fig. 2 shows a prospecting situation which has been modelled by Lee and Morrison, 1985, using the finite element method. Their results, as well as those from a program based on the SIE techniques as described herein, are shown in Figure 3. For the SIE solution, triangle basis functions were employed, together with point collation, the points being the contour partition midpoints. There were 50 such partitions, though convergence to within 8% of the anomaly values presented in Figure 3 for the quadrature component, and 40% for the (relatively small) real component can be realised with only 20 partitions. Field transforms were obtained at 10 wavenumber values before being inverse transformed (taking into account the symmetry with respect to wavenumber of the transformed fields) after cubic spline interpolation, though as few as 7 wavenumbers would have been good enough for 5% accuracy. CPU time was about 40 hours on a VAX11/780; however the program is at an early stage of development requiring much fine tuning, and this time could probably be reduced by a factor of 3 with little trouble.

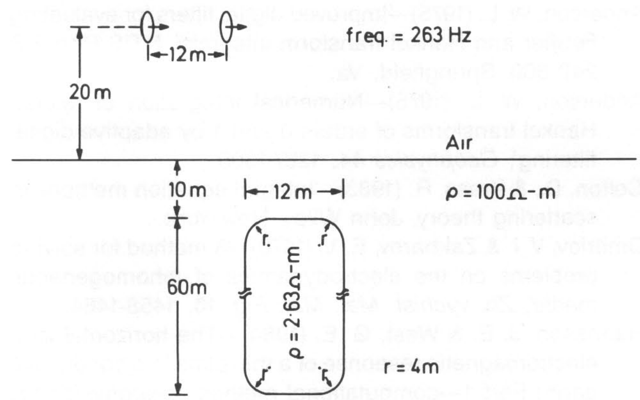

FIGURE 2
Model parameters for results shown in Fig. 5.

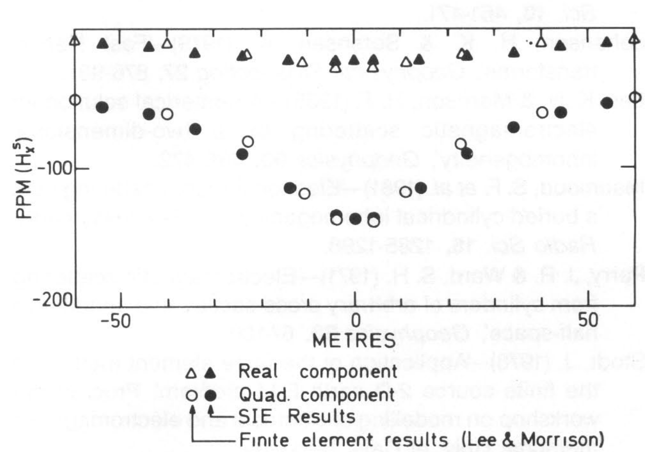

FIGURE 3
Comparison between SIE and finite element results for model of Fig. 2.

Conclusion

Little experience has, so far, been acquired by which to judge the strengths and weaknesses of the thick-body SIE method. However its performance seems to deteriorate at low frequencies as the matrix becomes ill-conditioned. This may be due to the fact that the surface divergences of $\underset{\sim}{a}$ and $\underset{\sim}{b}$ in eqns. (1)-(4) become more important than their actual values in meeting the boundary conditions. The next stage of development will attempt to better understand and redress this problem, and it is hoped that the increased flexibility in the choice of basis functions afforded by the one-dimensional nature of contour integration will aid in achieving success. Further development will also be aimed at modelling situations where the surface is not closed, e.g. an undulating base of the weathered layer.

The thick-body SIE method potentially offers great accuracy when source and/or receiver are close to an obstacle, by increasing the partitioning density where primary field and/or Green's function variations are greatest. In combination with the volume integral equation approach, it offers the power to model a range of realistic prospecting situations that cannot be modelled by either technique alone.

References

Anderson, W. L. (1975)—'Improved digital filters for evaluating Fourier and Hankel transform integrals', NTIS Rep. PB 242 800, Springfield, Va.

Anderson, W. L. (1975)—'Numerical integration of related Hankel transforms of orders 0 and 1 by adaptive digital filtering', *Geophysics* **44,** 1287-1305.

Colton, D., & Kress, R. (1983)—'Integral equation methods in scattering theory, John Wiley, New York.

Dmitriev, V. I. & Zakharov, E. V. (1970)—'A method for solving problems on the electrodynamics of inhomogeneous media', *Zh. vychist. Mat. Mat. Fig.* **10,** 1458-1464.

Hanneson, J. E. & West, G. E. (1984)—'The horizontal loop electromagnetic response of a thin plate in a conductive earth: Part 1—computational method', *Geophysics* **12,** 411-420.

Howard, A. Q. (1975)—'A canonical solution to the three-dimensional electromagnetic prospecting problem', *Radio Sci.* **10,** 461-471.

Johansen, H. K. & Sorensen, K. (1979)—'Fast Hankel transforms', *Geophysical Prospecting* **27,** 876-901.

Lee, K. H. & Morrison, H. F. (1985)—'A numerical solution for electromagnetic scattering by a two-dimensional inhomogeneity', *Geophysics* **50,** 466-472.

Mahmoud, S. F. *et al.* (1981)—'Electromagnetic scattering from a buried cylindrical inhomogeneity inside a lossy earth', *Radio Sci.* **16,** 1285-1298.

Parry, J. R. & Ward, S. H. (1971)—'Electromagnetic scattering from cylinders of arbitrary cross-section in a conductive half-space', *Geophysics* **36,** 67-100.

Stodt, J. (1978)—'Application of the finite element method to the finite source 2-D earth E-M problem', Proc. of the workshop on modelling of electrical and electromagnetic methods, Univ. of Calif. Berkeley.

Stoyer, C. H. & Greenfield, R. J. (1976)—'Numerical solutions of the reponse of two-dimensional earth to an oscillating magnetic source'. *Geophysics* **41,** 519-530.

Tabarovsky, L. A. (1975)—'Application of integral equation methods in the problems of geoelectrics', *Nauka*, Novosibirsk.

Tsubota, K. & Wait, J. R. (1980)—'The frequency and the time domain response of a buried axial conductor', *Geophysics* **45,** 941-951.

Wannamaker *et. al* (1984)—'Electromagnetic modelling of three-dimensional bodies in layered earths using integral equations', *Geophysics* **49,** 60-74.

Won, I. J. & Kuo, J. T. (1975)—'Representation theorems for multiregional electrodynamic diffraction: Part 1—Theory', *Geophysics* **40,** 96-108.

SIGNAL PROCESSING FOR CROSSHOLE SEISMIC IMAGING

R. D. Dowle and W. H. Holmes

Introduction

Boreholes are normally drilled on a wide grid pattern over potential coal mine sites to evaluate coal reserves, etc., but further drilling or geophysical methods are required for detailed coal seam mapping. Surface seismic methods are useful to find seam conditions without drilling, but are limited by the low frequencies used (< 150Hz even for high resolution surveys) to resolutions of the order of 10 m, which is inadequate for good mine planning. Higher frequencies cannot be transmitted through the surface soil and weathered layers.

The only way to overcome this problem is to position the seismic sources and receivers below the weathering. The method that has been developed at the University of N.S.W. uses a wideband marine seismic source (a sparker) and an array of hydrophone seismometer receivers in water-filled boreholes, as illustrated in Fig. 1 and described in more detail

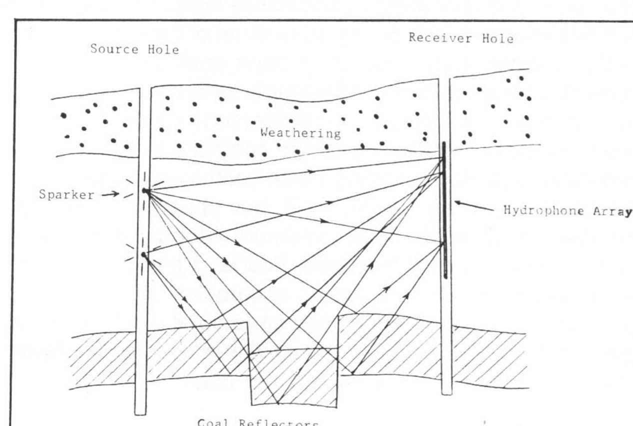

FIGURE 1
Diagram showing downhole-crosshole very high resolution coal seam profiling between boreholes.